







Article

Selective Inhibition of Heparan Sulphate and Not Chondroitin Sulphate Biosynthesis by a Small, Soluble Competitive Inhibitor

Marissa L. Maciej-Hulme ^{1,*},[†] , Eamon Dubaissi ², Chun Shao ³, Joseph Zaia ³ , Enrique Amaya ² , Sabine L. Flitsch ⁴ and Catherine L. R. Merry ^{1,*},[‡] 

¹ Materials Science Centre, School of Materials, The University of Manchester, Grosvenor St., Manchester M1 7HS, UK

² Division of Cell Matrix Biology & Regenerative Medicine, Faculty of Biology, Medicine and Health, Michael Smith Building, The University of Manchester, Oxford Road, Manchester M13 9PT, UK; eamon.dubaissi@manchester.ac.uk (E.D.); enrique.amaya@manchester.ac.uk (E.A.)

³ Center for Biomedical Mass Spectrometry, Boston University School of Medicine, 670 Albany Street, Boston, MA 02118, USA; Chun.Shao@bms.com (C.S.); jzaia@bu.edu (J.Z.)

⁴ School of Chemistry & Manchester Institute of Biotechnology, The University of Manchester, 131 Princess Street, Manchester M1 7DN, UK; Sabine.Flitsch@manchester.ac.uk

* Correspondence: marissa.maciej-hulme@radboudumc.nl (M.L.M.-H.); cathy.merry@nottingham.ac.uk (C.L.R.M.)

† Current address: Department of Nephrology, Radboudumc, Geert Grooteplein 10, 6525 GA Nijmegen, The Netherlands.

‡ Current address: Nottingham Biodiscovery Institute, School of Medicine, University of Nottingham, Nottingham NG7 2RD, UK.



Citation: Maciej-Hulme, M.L.; Dubaissi, E.; Shao, C.; Zaia, J.; Amaya, E.; Flitsch, S.L.; Merry, C.L.R. Selective Inhibition of Heparan Sulphate and Not Chondroitin Sulphate Biosynthesis by a Small, Soluble Competitive Inhibitor. *Int. J. Mol. Sci.* **2021**, *22*, 6988. <https://doi.org/10.3390/ijms22136988>

Academic Editors: Chiara Schiraldi, Donatella Cimini and Annalisa La Gatta

Received: 24 May 2021
Accepted: 19 June 2021
Published: 29 June 2021

Publisher's Note: MDPI stays neutral with regard to jurisdictional claims in published maps and institutional affiliations.



Copyright: © 2021 by the authors. Licensee MDPI, Basel, Switzerland. This article is an open access article distributed under the terms and conditions of the Creative Commons Attribution (CC BY) license (<https://creativecommons.org/licenses/by/4.0/>).

Abstract: The glycosaminoglycan, heparan sulphate (HS), orchestrates many developmental processes. Yet its biological role has not yet fully been elucidated. Small molecule chemical inhibitors can be used to perturb HS function and these compounds provide cheap alternatives to genetic manipulation methods. However, existing chemical inhibition methods for HS also interfere with chondroitin sulphate (CS), complicating data interpretation of HS function. Herein, a simple method for the selective inhibition of HS biosynthesis is described. Using endogenous metabolic sugar pathways, Ac₄GalNAz produces UDP-GlcNAz, which can target HS synthesis. Cell treatment with Ac₄GalNAz resulted in defective chain elongation of the polymer and decreased HS expression. Conversely, no adverse effect on CS production was observed. The inhibition was transient and dose-dependent, affording rescue of HS expression after removal of the unnatural azido sugar. The utility of inhibition is demonstrated in cell culture and in whole organisms, demonstrating that this small molecule can be used as a tool for HS inhibition in biological systems.

Keywords: heparan sulfate; azido sugar; glycosaminoglycan; carbohydrate biosynthesis; small molecule inhibitor; biorthogonal chemistry

1. Introduction

Heparan sulphate (HS) is a prevalent glycosaminoglycan (GAG) attached to protein cores (proteoglycans) on the cell surface of almost every cell type. HS proteoglycans form an integral part of the extracellular matrix with important roles in development [1], homeostasis [2,3] and disease [4,5]. HS is involved in cell-cell and cell-matrix communication, fine-tuning cellular responses to the extracellular milieu.

HS biosynthesis consists of a repeating disaccharide unit structure of glucuronic acid-*N*-acetylglucosamine (GlcA-GlcNAc) polymerised by the exostoses enzyme complex (EXT1/2) from UDP-GlcA and UDP-GlcNAc active nucleotide donor sugars [6–8]. During this process the *N*-deacetylase/*N*-sulphotransferase (NDST) enzymes work in tandem to begin modification of the nascent chain. The NDST enzymes can replace the acetyl group

on GlcNAc with a sulphate [9], often providing the gateway step for further modifications of the chain. Additionally, the NDSTs are also involved in control of HS chain length [10] with NDST shown to be co-localised with EXT2 [11]. During extension of the backbone, several other chemical modifications are possible, resulting in fine patterning of the chain where the functionality of HS is encoded. O-sulphotransferases (OSTs) modify the HS chain at the 2-, 6- and 3-O position or epimerisation of GlcA to iduronic acid (IdoA) by C5-epimerase can occur. Together, these enzymes contribute to HS functionality by influencing the fine patterning of the chain [12].

Despite its widespread role in biology, few chemical tools exist for the manipulation of HS function, with those available often interfering with chondroitin sulphate/dermatan sulphate (CS/DS) pathways simultaneously. Methods to ablate HS exist via targeted genetic deletion of biosynthetic HS enzymes [6,7]. However, genetic manipulation is costly and labour intensive with embryonic lethality in null mutant animals [7], posing challenges for post-embryonic analysis. In contrast, chemical approaches offer cheap, user-friendly alternatives, which either perturb sulphation of the chain [13,14] or compete with endogenous substrates involved in HS assembly, such as amino sugar derivatives [15,16] and mimics of tetrasaccharide linkages [17–20]. However, the additional effect on CS/DS synthesis can complicate data interpretation particularly when both GAGs are displayed on the proteoglycan of interest [21].

Azido sugars and other bio-orthogonal chemistry approaches have been demonstrated as useful functionalised chemical probes to label *N*-glycans [22], O-GlcNAc modifications [23], mucin type O-GalNAc glycans [24] and sialic acid moieties [25]. Tetra-acetylated *N*-azidoacetylgalactosamine (Ac₄GalNAz) can be metabolically converted to UDP-GlcNAz and UDP-GalNAz via the GalNAc salvage pathway [23], potentiating its use in GAG synthesis (Figure 1).

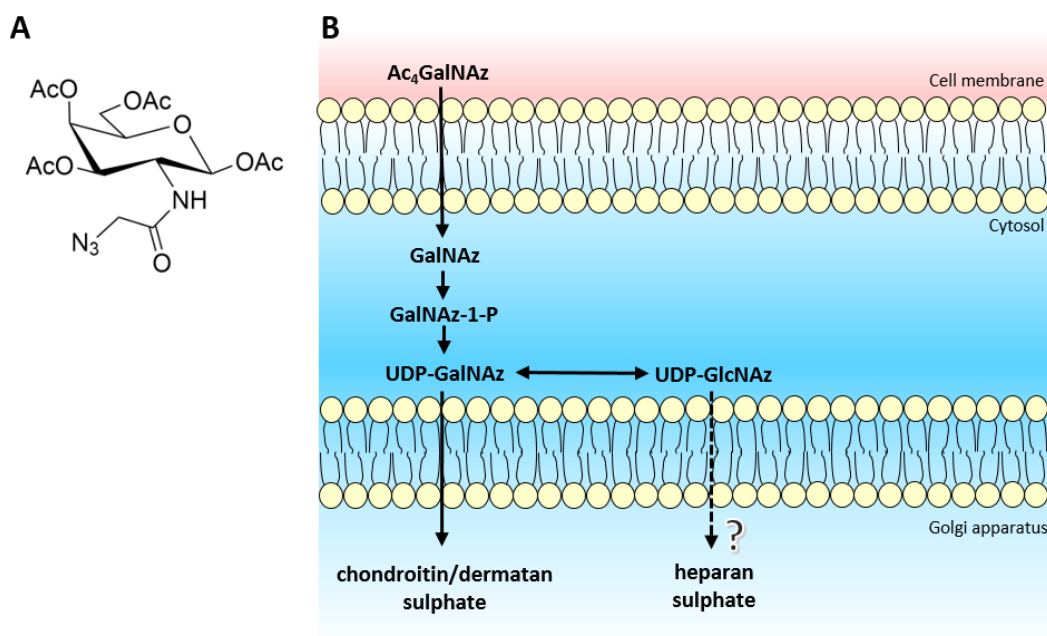


Figure 1. (A) Structure of tetra-acetylated *N*-azidoacetylgalactosamine. (B) Schematic of biological azido sugar precursor production for GAG synthesis. Ac₄GalNAz travels across the cell membrane and enters the cytoplasm. Endogenous deacetylases remove the acetyl protective groups leaving GalNAz, ready to enter the GalNAc salvage pathway. After a cascade of enzymes, both UDP-GalNAz and UDP-GlcNAz are produced, which target CS/DS and potentially HS biosynthesis respectively.

The azido sugar nucleotide donors mimic UDP-GalNAc and UDP-GlcNAc, required for CS/DS and HS biosynthesis respectively. Recently, the EXT1/2 enzyme complex has been shown to utilise UDP-GlcNAz as a substrate for the addition of GlcNAz to the

non-reducing termini of heparan sulphate chains *in vitro* [26]. However *in vivo*, there is the potential that UDP-GlcNAz could interfere with the interaction or activity of the HS polymerisation machinery (EXT/NDST enzymes) due to the location of the azido group situated on the acetyl position of the GlcNAc residue, thereby producing an inhibitory effect on the biosynthetic pathway. Therefore, we sought to extend and validate the use of Ac₄GalNAz treatment as a potential novel, small chemical inhibitor of HS synthesis.

2. Results and Discussion

Chinese hamster ovary (CHO) cells were treated with different concentrations (7–35 μ M) of Ac₄GalNAz. No lethal effect on the cells was observed. Cell surface HS was analysed using flow cytometry. A reduction in anti-(10E4) HS antibody staining was observed at the cell surface in response to increasing Ac₄GalNAz concentration (Figure 2).

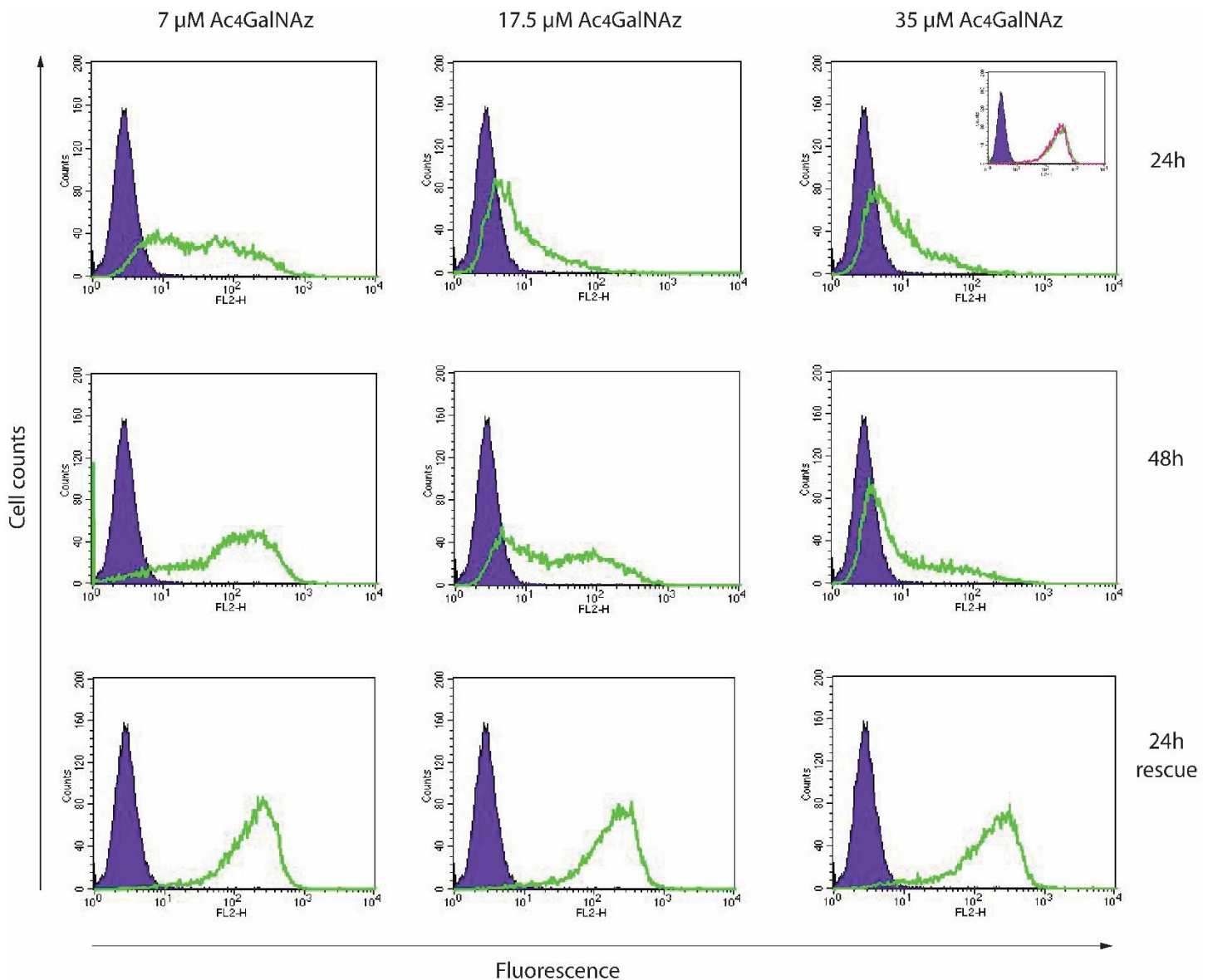


Figure 2. Flow cytometric analysis of Ac₄GalNAz-treated CHOs. Cells were treated with 7–35 μ M Ac₄GalNAz for 24–48 h, or for the first 24 h, then 24 h without Ac₄GalNAz (24 h rescue) and analysed for cell surface anti-HS (10E4) reactivity. Purple infilled, antibody control. Green trace, Ac₄GalNAz-treated cells. Inset, experimental controls: purple infilled, antibody control; green trace, vehicle-treated; pink trace, untreated.

To sustain the reduction of HS for longer periods, higher concentrations (35 μM) of azido sugar were required. Both 7 μM and 17.5 μM gave partial population decreases in 10E4 staining and removal of Ac_4GalNAz returned HS expression levels to match untreated cell populations (24 h rescue), indicating that the effect of the azido sugar treatment on HS was transient and reversible. Significantly less HS was present in 35 μM Ac_4GalNAz conditions compared with vehicle control conditions with HS depletion displaying a significant dose-dependent decrease (Figure 3A).

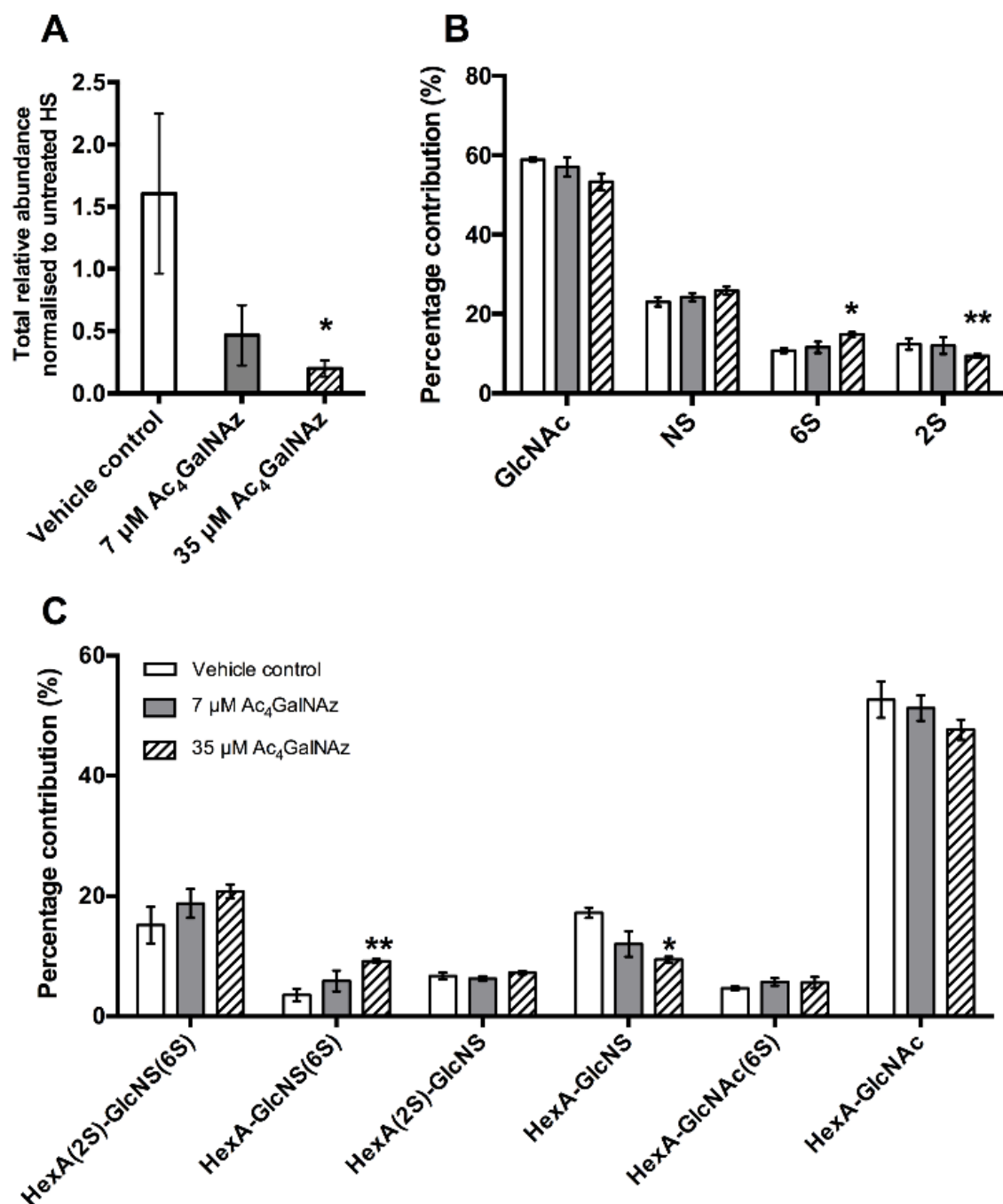


Figure 3. (A). Total relative abundance of HS from cell extracted samples. (B) Percentage chemical modification contribution of HS and (C) percentage contribution of HS disaccharide species after RP-HPLC separation of 2-AMAC-tagged HS. Error bars represent SEM of $N = 3$ independent experiments. * $p \leq 0.05$, ** $p \leq 0.01$, student's t test (two tailed). HexA, hexuronic acid (iduronic or glucuronic acid); 2S, 2-O-sulphate; 6S, 6-O-sulphate; NS, N-sulphate.

Furthermore, HS biosynthesis was perturbed as a subtle, but significant change in disaccharide composition (Figure 3B,C) showing alterations in the sulphation of the chain (increase in 6-O-sulphation and decrease 2-O-sulphation), reminiscent of GAG biosynthetic enzyme mutants [27,28]. To elucidate changes in HS chain length, CHO cell cultures were radiolabelled with ^3H -glucosamine alongside treatment with Ac_4GalNAz and HS populations from cell extracts were purified as previously described [29]. Total GAG synthesis was normalised to protein level. Radiolabelled studies showed a dose dependent decrease in the quantity (Figure 4) and chain length of HS (Table 1) in Ac_4GalNAz -treated cells compared to control.

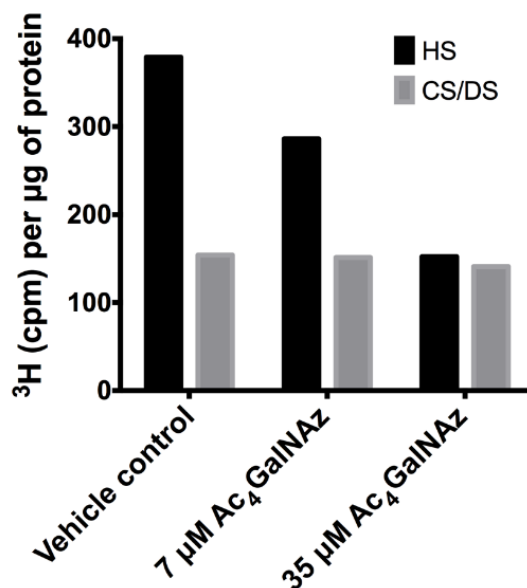


Figure 4. Total GAG synthesis normalised to protein levels from CHO-K1 cells.

Table 1. Chain length of radiolabelled HS and CS/DS.

Condition	Secreted Modal Size (kDa)		Cell Extract Modal Size (kDa)	
	HS	CS/DS	HS	CS/DS
Vehicle control	22	32	8.5	38
7 μM Ac_4GalNAz	12	22	6.9	31
35 μM Ac_4GalNAz	7	32	7.5	32

The marked decrease in chain length observed in both secreted HS and cell-derived HS populations after Ac_4GalNAz treatment (Table 1) suggests that early termination of chain synthesis was responsible for the depletion of HS at the cell surface observed in flow cytometric experiments (Figure 2).

Despite significant changes to HS chain synthesis, no incorporation of azido groups was detected in HS chains (data not shown), suggesting that either GlcNAz was not incorporated into the chain or that the azide was potentially removed by NDST activity during HS synthesis.

Due to convergence in their synthetic pathways (Figure 1) and the utilisation of common precursors, chemical inhibitors usually affect both HS and CS/DS GAGs indiscriminately, therefore we assessed whether CS/DS synthesis was also inhibited by the same metabolic labelling strategy. Azido sugar labelling of CS proteoglycans using GalNAz has been described previously [30,31], but examination of the biosynthesis of CS/DS was not reported. No changes in CS/DS composition (Figure 5), chain length (Table 1) or quantity were observed (Figure 4), suggesting that the inhibitory effect of Ac_4GalNAz treatment was specific to HS synthesis.

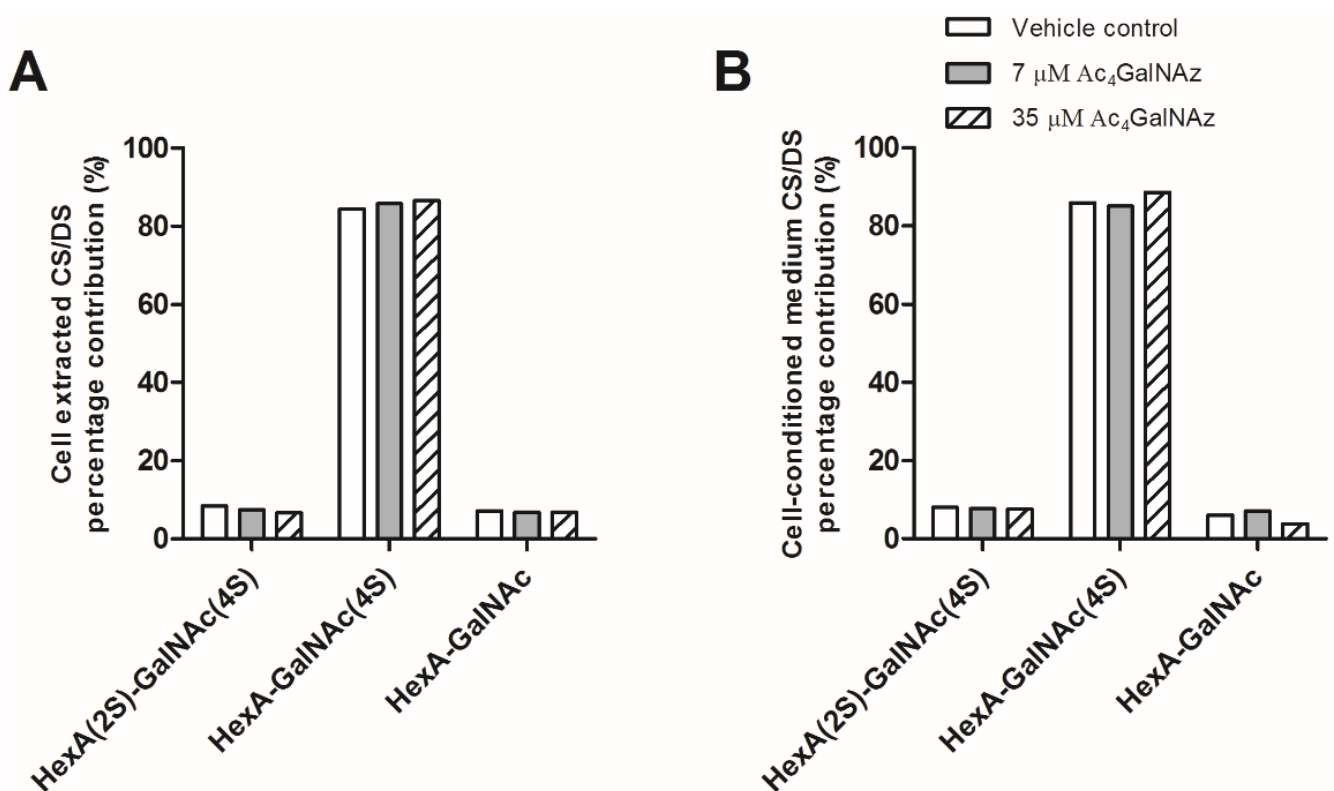


Figure 5. CS/DS disaccharide analysis from (A) CHO-K1 cell extracts and (B) cell-conditioned medium. Percentage contribution of CS/DS disaccharide species after SAX-HPLC of radiolabelled preparations. Other CS/DS disaccharide species were not detected. HexA, hexuronic acid (iduronic or glucuronic acid). 4S, 4-O-sulphate; 2S, 2-O-sulphate.

Ac₄ManNAz has also been reported to label CS proteoglycans, however the presence of CS-specific labelling on the proteoglycan was not investigated [32]. Notably, no NDST enzymes are associated with CS/DS synthesis and the acetyl group of GalNAc remains unmodified, whereas HS biosynthesis specifically involves removal of the acetyl and *N*-sulphation of GlcNAc. This process, at least in part, controls HS chain length [11] possibly via NDST interaction with EXT co-polymerase, although the mechanism is still unclear. EXT enzyme activity *in vitro* has been demonstrated to utilise UDP-GlcNAz as a substrate [26], suggesting that extension of the HS chain by the EXTs is likely to remain unaffected by GlcNAz *in vivo*. Thus, we hypothesise that the presence of GlcNAz interferes with normal NDST function, thereby inhibiting HS synthesis and resulting in truncated HS chains. Importantly, upregulation of NDST1 has been associated with chemoresistance in breast cancer [33] and upregulated NDST1 activity increases HS biosynthesis [11]. Thus, selective strategies for inhibition of HS activity, such as this one, may have therapeutic potential alongside current treatment options where HS is a known driver of chemoresistance and/or tumour growth.

Finally, since HS has been also demonstrated to play important roles in development [1], we sought to test the ability of the azido sugar to inhibit HS in a model organism. Therefore, a well-characterised and widely used developmental biology vertebrate model (*Xenopus tropicalis*) was utilised [34]. Following treatment with the inhibitor, the abundance of total HS in Ac₄GalNAz-treated embryos was decreased compared with controls (Figure 6A), confirming that this small, soluble inhibitor can be used in both organismal and cell culture-based experiments to inhibit HS synthesis.

The Ac₄GalNAz-treated *Xenopus* embryos displayed a phenotypic short stature (Figure 6B) accompanied with irregular somite boundaries and abnormal skeletal muscle orientation in a dose dependent manner, resulting in gross disorganization of the tail structure and tail kinks (Supplementary Figure S1).

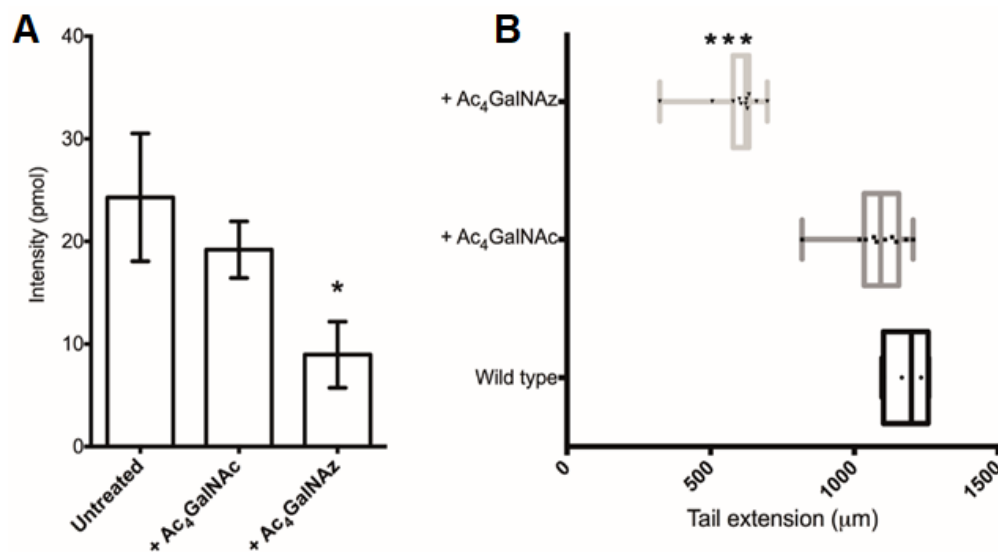


Figure 6. Ac₄GalNAz treatment of *Xenopus* embryos. **(A)** Total HS (pmol) per embryo. **(B)** Embryo stature measurements of the tail extension (µm). + Ac₄GalNAz, 500 pmol injection and 500 µM soaking; + Ac₄GalNAc, 500 pmol injection and 500 µM soaking. * $p \leq 0.05$, *** $p \leq 0.001$ + Ac₄GalNAz vs. Wildtype. Oneway ANOVA with Turkey post-hoc comparison.

Interestingly, similar developmental abnormalities have been observed in UDP-4-azido-4-deoxyxylose-treated zebrafish [17], where GAG synthesis (CS and HS) was broadly targeted, preventing elongation of either type of GAG. Targeted application of Ac₄GalNAz as a small, selective HS inhibitor thus provides independent evaluation of the role of HS in biological systems where transient knock down of HS biosynthesis is desired.

3. Conclusions

We propose that a common sugar analogue, Ac₄GalNAz, can be applied as a small, soluble and reversible chemical inhibitor of HS, which does not affect CS/DS biosynthesis, offering a new tool for HS inhibition. Ac₄GalNAz can be synthesised from inexpensive compounds [35] and is commercially available. Using this strategy, HS inhibition can be achieved in cell-based assays and in whole organisms. The effect of Ac₄GalNAz on HS production is transient (Figure 2), enabling flexible application and removal in experiments without the need for gene manipulation. This novel selective HS inhibitor therefore may be used to probe HS biology in separation from CS/DS to identify HS-mediated mechanisms in biological systems for further investigation.

4. Materials and Methods

4.1. Cell Culture, Ac₄GalNAz and D-[6-³H]-Glucosamine Treatment

Chinese Hamster Ovary-K1 (CHO-K1) cells (gifted from the Esko lab) were cultured at 37 °C/5% CO₂ humidified conditions in Dulbecco's Modified Eagle Medium: F12 Nutrient Mix (Ham) media (Invitrogen, Loughborough, UK) supplemented with 10% *v/v* fetal bovine serum (FBS) (batch-tested, Biosera) and 2 mM L-glutamine (PAA). Cell culture medium was supplemented with sugars dissolved in dimethylsulfoxide (DMSO): Ac₄GalNAz (Molecular Probes, Loughborough, UK), Ac₄GalNAc (gifted from the Flitsch group). For radioactive experiments, CHO medium was supplemented with 50 µCi D-[6-³H]-glucosamine hydrochloride (Perkin Elmer, Llantrisant, UK). CHO-K1 cells were seeded at 40,000 cells/cm² and then cultured for 48 h for metabolic incorporation of the radiolabelled sugar.

4.2. Flow Cytometry

To preserve the cell surface, non-enzymatic cell dissociation buffer (Gibco, Loughborough, UK) was used to remove CHO cells from tissue culture plastic. After washing with phosphate buffered saline (PBS), cells were incubated with anti-HS (F58–10E4) (1:200, Amsbio, Abingdon, UK) in 0.2% (*w/v*) bovine serum albumin (BSA), followed by AlexaFluor goat anti-mouse IgM (κ)-488 (1:1000, Molecular Probes, Loughborough, UK). Cells were fixed with 1% PFA for 10 min at room temperature before analysis on a Cyan ADP cytometer (Beckman Coulter, High Wycombe, UK) using CellQuest Pro software).

4.3. GAG Collection and Purification

Cell membranes were dispersed with 1% Triton X-100 in PBS with gentle agitation for 1–2 h. Proteins were digested with 100 $\mu\text{g}/\text{mL}$ Pronase (*Streptomyces griseus*, Roche, Welwyn Garden City, UK) for 4 h at 37 °C. Diethylaminoethyl (DEAE) anion-exchange chromatography for GAG preparations with step elution of HS and CS/DS using 1.5 M NaCl was used to isolate GAG material as previously described [36], with the exception of the radiolabelled GAG preparations where gradient anion exchange chromatography (0–1.5 M NaCl) was used. GAG samples were desalted using PD10 columns (GE Healthcare, Amersham, UK) and lyophilised.

4.4. HS and CS Chain Length Analysis

Purified D-[6-³H]-radiolabelled HS or CS material was treated with 50 mM NaOH/1 M NaBH₄ at 45 °C for 48 h to cleave the protein stub from the xylose residue. Samples were neutralized with glacial acetic acid and then separated on Sepharose CL-6B columns in 0.2 M ammonium bicarbonate at a flow rate of 0.2 mL/min. 1 mL fractions were collected in pony vials (Sigma, Gillingham, UK) and 2 mL Optimax scintillation fluid (Perkin Elmer, Llantrisant, UK) was added. Samples were sealed and shaken before processing for ³H radioactivity (counts per minutes) using a liquid scintillation counter (Wallac 1409, Beckman Coulter, High Wycombe, UK). Modal chain length was estimated by comparison of K_{av} values with a calibration curve [37].

4.5. Generation of GAG Disaccharide Species

Purified GAG samples were digested either with 2 mIU of each heparinase I–III (Iduron) in 0.1 M sodium acetate, 0.1 mM calcium acetate, pH 7.0 or with chondroitinase ABC (Amsbio, Abingdon, UK) in 50 mM Tris, 50 mM NaCl, pH 7.9 for 16 h at 37 °C. For radiolabelled preparations, the disaccharides were separated from oligosaccharides via Superdex-30 chromatography.

4.6. 2-AMAC Labelling and RP-HPLC Separation of HS Disaccharides

HS disaccharides were labelled with 2-aminoacridone (2-AMAC) and separated using RP-HPLC as previously described using correction factors for the batch of 2-AMAC utilised [38,39]. Data was also used to calculate the HS sulphation modification.

4.7. Strong Anion Exchange (SAX)-HPLC Separation of CS Disaccharides

Samples of 5000 cpm digested D-[6-³H]-CS disaccharides were separated on a Hypersil 5 μm SAX column (Thermo Scientific, Loughborough, UK) with a gradient of 0.15 M–0.7 M NaCl pH 3.5 over 47 min at a flow rate of 1 mL/min.

4.8. Sugar Microinjection and Incubation of *Xenopus* Embryos

Fertilised NF stage 1 embryos in injection buffer (1% (*w/v*) Ficoll in 0.1 \times Modified Marc Ringers, (MMR), pH 8.0) were injected with 1–5 nL of 500–1000 picomoles Ac₄GalNAz or Ac₄GalNAc (dissolved in 0.2 mM KCl) into the cytoplasm using a heat-pulled borosilicate glass capillary injection needle (1 mm \times 0.78 mm, Harvard apparatus, Holliston, MA, USA). Embryos were left to recover in injection buffer for 1–2 h (stage 7–8) at 28 °C before they were transferred to fresh agarose-coated dishes containing a bath of 0–500 μM Ac₄GalNAz

or Ac₄GalNAc in 0.01 × MMR solution. Embryos were incubated at 23 °C (prior to gastrulation) for the first day of development, then at 25 °C and transferred to fresh sugar/0.01 × MMR conditions daily.

4.9. Purification of *Xenopus* HS

Embryos were lyophilised and ground in a pestle and mortar with 1 mL of PBS before addition of 1 mg/mL Pronase in 50 mM Tris/HCl pH 8.0, 1 mM CaCl₂, 1% Triton X-100. Proteins were digested for 16 h at 55 °C, then a further 0.5 mg Pronase was added and the digestion continued overnight. Pronase was heat-inactivated at 100 °C for 10 min and samples were then treated with 2 µL of 2 M MgCl₂ and 0.5 µL Benzonase Nuclease (300 mU, Sigma, Gillingham, UK) at 37 °C for 3 h before adjustment to 0.5 M NaOH and mixing overnight. Formic acid was used to adjust the pH to 5.0 prior to centrifugation at 13,000 rpm. The supernatant was diluted with HPLC grade water and applied to DEAE anion exchange chromatography as described in [36] with the following alterations: DEAE beads were washed only with HPLC grade water prior to sample application and samples were eluted with 1 M NaCl, 20 mM NaOAc pH 6.0. The eluent was desalted using PD10 columns according to the manufacturer's instructions.

4.10. Mass Spectrometry Analysis of *Xenopus* HS Disaccharides

Xenopus HS disaccharides were diluted in 200 µL HPLC grade water and centrifuged at 12,000 rpm for 10 min to remove insoluble material. Residual salts and/or proteins were removed from the supernatant using size-exclusion chromatography (Beckman SEC offline fractionate), followed by further clean up using a porous graphite carbon C-18 TopTip (Glygen) prior to Liquid Chromatography-Mass Spectrometry using a Dionex GlycanPac AXH-1 (1 mm × 15 cm) (ThermoFisher, Walton, MA, USA) on an Agilent QTOF 6520 in negative mode, with an acquisition range of 100–1700 *m/z*. Heparin disaccharide I-P sodium salt (ΔUA2S-GlcNCOEt6S) (V-labs, Dextra Laboratories, Reading, UK) was spiked into all samples as an external standard to monitor the spray conditions and used for normalization between samples.

4.11. Whole Mount Antibody Fluorescent Imaging

Embryos were fixed in 0.1 M 3-(N-Morpholino)propane sulfonic acid (MOPS) pH 7.4, 2 mM ethylene glycol-bis(β-aminoethyl ether)-N,N,N',N'-tetraacetic acid (EGTA), 1 mM MgSO₄, 3.7% (*v/v*) formaldehyde for 16 h at 4 °C before dehydration with 100% methanol. Embryos were then rehydrated by gradient dilution of the methanol with H₂O and antibody staining was performed as previously described [40] using mouse 12/101 IgG₁ (1:200, Developmental Studies Hybridoma Bank) followed by AlexaFluor goat anti-mouse IgG (H + L)-594 (1:500, Molecular Probes). Embryos were imaged using a glass-bottomed dish (MatTek Corporation, Bratislava, Slovakia) and imaged by confocal microscopy using an Olympus Fluoview FV1000 (Olympus, Southend-on-Sea, UK).

Supplementary Materials: The following are available online at <https://www.mdpi.com/article/10.3390/ijms22136988/s1>, Figure S1: Wholmount fluorescence of skeletal muscle in stage 39 NF *Xenopus tropicalis* tadpoles after the injection of sugars.

Author Contributions: M.L.M.-H., C.L.R.M.; Methodology: M.L.M.-H.; Validation: M.L.M.-H., C.S.; Formal analysis: M.L.M.-H.; Investigation: M.L.M.-H., C.S., E.D.; Writing—original draft: M.L.M.-H.; Writing—review & editing: M.L.M.-H., C.L.R.M., S.L.F., E.A., E.D., J.Z., C.S.; Supervision: J.Z., S.L.F., E.A., C.L.R.M.; Project administration: C.L.R.M.; Funding acquisition: E.A., C.L.R.M. All authors have read and agreed to the published version of the manuscript.

Funding: This work was supported by a BBSRC DTC Studentship Grant No. 978724 and MRC grant (MR/L007525/1).

Institutional Review Board Statement: Experiments involving *Xenopus* embryos were approved by the local ethics committee and the Home Office (PPL 70/7648).

Informed Consent Statement: Not applicable.

Acknowledgments: The authors would like to thank Robert Lea for technical support throughout the generation of the *Xenopus* data, Santanu Mandal for per-acetylation of GalNAc (Ac₄GalNAc) and Jeffrey Esko for the CHO-K1 cells.

Conflicts of Interest: The authors declare no conflict of interest. The funders had no role in the design of the study; in the collection, analyses, or interpretation of data; in the writing of the manuscript, or in the decision to publish the results.

References

1. Hacker, U.; Nybakken, K.; Perrimon, N. Heparan sulphate proteoglycans: The sweet side of development. *Nat. Rev. Mol. Cell Biol.* **2005**, *6*, 530–541. [[CrossRef](#)] [[PubMed](#)]
2. Wrenshall, L.E.; Platt, J.L. Regulation of T cell homeostasis by heparan sulfate-bound IL-21. *J. Immunol.* **1999**, *163*, 3793–3800. [[PubMed](#)]
3. Coulson-Thomas, V.J.; Gesteira, T.F.; Esko, J.; Kao, W. Heparan sulfate regulates hair follicle and sebaceous gland morphogenesis and homeostasis. *J. Biol. Chem.* **2014**, *289*, 25211–25226. [[CrossRef](#)] [[PubMed](#)]
4. Lindahl, U.; Kjellen, L. Pathophysiology of heparan sulphate: Many diseases, few drugs. *J. Intern. Med.* **2013**, *273*, 555–571. [[CrossRef](#)] [[PubMed](#)]
5. Gomes, A.M.; Stelling, M.P.; Pavao, M.S.G. Heparan sulfate and heparanase as modulators of breast cancer progression. *Biomed Res. Int.* **2013**, 1–11. [[CrossRef](#)]
6. Lin, X.; Wei, G.; Shi, Z.; Dryer, L.; Esko, J.D.; Wells, D.E.; Matzuk, M.M. Disruption of gastrulation and heparan sulfate biosynthesis in EXT1-deficient mice. *Dev. Biol.* **2000**, *224*, 299–311. [[CrossRef](#)] [[PubMed](#)]
7. Stickens, D.; Zak, B.M.; Rougier, N.; Esko, J.D.; Werb, Z. Mice deficient in Ext2 lack heparan sulfate and develop exostoses. *Development* **2005**, *132*, 5055–5068. [[CrossRef](#)]
8. McCormick, C.; Duncan, G.; Goutsos, K.T.; Tufaro, F. The putative tumor suppressors EXT1 and EXT2 form a stable complex that accumulates in the Golgi apparatus and catalyzes the synthesis of heparan sulfate. *Proc. Natl. Acad. Sci. USA* **2000**, *97*, 668–673. [[CrossRef](#)]
9. Bengtsson, J.; Eriksson, I.; Kjellen, L. Distinct effects on heparan sulfate structure by different active site mutations in NDST-1. *Biochemistry* **2003**, *42*, 2110–2115. [[CrossRef](#)]
10. Deligny, A.; Dierker, T.; Dagälv, A.; Lundequist, A.; Eriksson, I.; Nairn, A.V.; Moremen, K.W.; Merry, C.L.; Kjellén, L. NDST2 (N-Deacetylase/N-Sulfotransferase-2) enzyme regulates heparan sulfate chain length. *J. Biol. Chem.* **2016**, *291*, 18600–18607. [[CrossRef](#)]
11. Presto, J.; Thuveson, M.; Carlsson, P.; Busse, M.; Wilén, M.; Eriksson, I.; Kusche-Gullberg, M.; Kjellén, L. Heparan sulfate biosynthesis enzymes EXT1 and EXT2 affect NDST1 expression and heparan sulfate sulfation. *Proc. Natl. Acad. Sci. USA* **2008**, *105*, 4751–4756. [[CrossRef](#)]
12. Sasisekharan, R.; Venkataraman, G. Heparin and heparan sulfate: Biosynthesis, structure and function. *Curr. Opin. Chem. Biol.* **2000**, *4*, 626–631. [[CrossRef](#)]
13. Dietrich, C.P.; Nader, H.B.; Buonassisi, V.; Colburn, P. Inhibition of synthesis of heparan sulfate by selenate—Possible dependence on sulfation for chain polymerization. *FASEB J.* **1988**, *2*, 56–59. [[CrossRef](#)]
14. Greve, H.; Cully, Z.; Blumberg, P.; Kresse, H. Influence of chlorate on proteoglycan biosynthesis by cultured human fibroblasts. *J. Biol. Chem.* **1988**, *263*, 12886–12892. [[CrossRef](#)]
15. Kisilevsky, R.; Szarek, W.A.; Ancsin, J.B.; Elimova, E.; Marone, S.; Bhat, S.; Berkin, A. Inhibition of amyloid A amyloidogenesis in vivo and in tissue culture by 4-deoxy analogues of peracetylated 2-acetamido-2-deoxy- α - and β -D-glucose—Implications for the treatment of various amyloidoses. *Am. J. Pathol.* **2004**, *164*, 2127–2137. [[CrossRef](#)]
16. Van Wijk, X.M.R.; Oosterhof, A.; van den Broek, S.A.; Griffioen, A.W.; Gerdy, B.; Rutjes, F.P.; van Delft, F.L.; van Kuppevelt, T.H. A 4-deoxy analogue of N-acetyl-D-glucosamine inhibits heparan sulphate expression and growth factor binding in vitro. *Exp. Cell Res.* **2010**, *316*, 2504–2512. [[CrossRef](#)]
17. Beahm, B.J.; Dehnert, K.W.; Derr, N.L.; Kuhn, J.; Eberhart, J.K.; Spillmann, D.; Amacher, S.L.; Bertozzi, C.R. A Visualizable chain-terminating inhibitor of glycosaminoglycan biosynthesis in developing zebrafish. *Angew. Chem. Int. Ed.* **2014**, *53*, 3347–3352. [[CrossRef](#)]
18. Kanwar, Y.S.; Hascall, V.C.; Jakubowski, M.L.; Gibbons, J.T. Effect of beta-D-xyloside on the glomerular proteoglycans. 1. Biochemical-studies. *J. Cell Biol.* **1984**, *99*, 715–722. [[CrossRef](#)]
19. Garud, D.R.; Tran, V.M.; Victor, X.V.; Koketsu, M.; Kuberan, B. Inhibition of heparan sulfate and chondroitin sulfate proteoglycan biosynthesis. *J. Biol. Chem.* **2008**, *283*, 28881–28887. [[CrossRef](#)]
20. Tsuzuki, Y.; Nguyen, T.K.N.; Garud, D.R.; Kuberan, B.; Koketsu, M. 4-Deoxy-4-fluoro-xyloside derivatives as inhibitors of glycosaminoglycan biosynthesis. *Bioorganic Med. Chem. Lett.* **2010**, *20*, 7269–7273. [[CrossRef](#)]
21. Esko, J.D.; Lindahl, U. Molecular diversity of heparan sulfate. *J. Clin. Investig.* **2001**, *108*, 169–173. [[CrossRef](#)] [[PubMed](#)]
22. Breidenbach, M.A.; Gallagher, J.E.; King, D.S.; Smart, B.P.; Wu, P.; Bertozzi, C.R. Targeted metabolic labeling of yeast N-glycans with unnatural sugars. *Proc. Natl. Acad. Sci. USA* **2010**, *107*, 3988–3993. [[CrossRef](#)] [[PubMed](#)]

23. Boyce, M.; Carrico, I.S.; Ganguli, A.S.; Yu, S.H.; Hangauer, M.J.; Hubbard, S.C.; Kohler, J.J.; Bertozzi, C.R. Metabolic cross-talk allows labeling of O-linked beta-N-acetylglucosamine-modified proteins via the N-acetylgalactosamine salvage pathway. *Proc. Natl. Acad. Sci. USA* **2011**, *108*, 3141–3146. [[CrossRef](#)] [[PubMed](#)]
24. Debets, M.F.; Tasthan, O.Y.; Wisnovsky, S.P.; Malaker, S.A.; Angelis, N.; Moeckl, L.K.; Choi, J.; Flynn, H.; Wagner, L.J.; Bineva-Todd, G.; et al. Metabolic precision labeling enables selective probing of O-linked N-acetylgalactosamine glycosylation. *Proc. Natl. Acad. Sci. USA* **2020**, *117*, 25293–25301. [[CrossRef](#)]
25. Yang, L.F.; Nyalwidhe, J.O.; Guo, S.; Drake, R.R.; Semmes, O.J. Targeted Identification of Metastasis-associated Cell-surface Sialoglycoproteins in Prostate Cancer. *Mol. Cell. Proteom.* **2011**, *10*, M110.007294. [[CrossRef](#)]
26. Wu, Z.L.; Huang, X.; Ethen, C.M.; Tatge, T.; Pasek, M.; Zaia, J. Non-reducing end labeling of heparan sulfate via click chemistry and a high throughput ELISA assay for heparanase. *Glycobiology* **2017**, *27*, 518–524. [[CrossRef](#)]
27. Merry, C.L.R.; Bullock, S.L.; Swan, D.C.; Backen, A.C.; Lyon, M.; Beddington, R.S.; Wilson, V.A.; Gallagher, J.T. The molecular phenotype of heparan sulfate in the Hs2st(-/-) mutant mouse. *J. Biol. Chem.* **2001**, *276*, 35429–35434. [[CrossRef](#)]
28. Bai, X.M.; Esko, J.D. An animal cell mutant defective in heparan sulfate hexuronic acid 2-O-sulfation. *J. Biol. Chem.* **1996**, *271*, 17711–17717. [[CrossRef](#)]
29. Merry, C.L.; Lyon, M.; Deakin, J.A.; Hopwood, J.J.; Gallagher, J.T. Highly sensitive sequencing of the sulfated domains of heparan sulfate. *J. Biol. Chem.* **1999**, *274*, 18455–18462. [[CrossRef](#)]
30. Laughlin, S.T.; Bertozzi, C.R. In vivo imaging of caenorhabditis elegans glycans. *ACS Chem. Biol.* **2009**, *4*, 1068–1072. [[CrossRef](#)]
31. Hang, H.C.; Yu, C.; Kato, D.L.; Bertozzi, C.R. A metabolic labeling approach toward proteomic analysis of mucin-type O-linked glycosylation. *Proc. Natl. Acad. Sci. USA* **2003**, *100*, 14846–14851. [[CrossRef](#)]
32. Loebel, C.; Kwon, M.Y.; Wang, C.; Han, L.; Mauck, R.L.; Burdick, J.A. Metabolic Labeling to Probe the Spatiotemporal Accumulation of Matrix at the Chondrocyte-Hydrogel Interface. *Adv. Funct. Mater.* **2020**, *30*, 1909802. [[CrossRef](#)]
33. He, D.X.; Gu, X.T.; Li, Y.R.; Jiang, L.; Jin, J.; Ma, X. Methylation-regulated miR-149 modulates chemoresistance by targeting GlcNAc N-deacetylase/N-sulfotransferase-1 in human breast cancer. *FEBS J.* **2014**, *281*, 4718–4730. [[CrossRef](#)]
34. Amaya, E.; Offield, M.F.; Grainger, R.M. Frog genetics: *Xenopus tropicalis* jumps into the future. *Trends Genet.* **1998**, *14*, 253–255. [[CrossRef](#)]
35. Laughlin, S.T.; Bertozzi, C.R. Metabolic labeling of glycans with azido sugars and subsequent glycan-profiling and visualization via Staudinger ligation. *Nat. Protoc.* **2007**, *2*, 2930–2944. [[CrossRef](#)]
36. Guimond, S.E.; Puvirajesinghe, T.M.; Skidmore, M.A.; Kalus, I.; Dierks, T.; Yates, E.A.; Turnbull, J.E. Rapid purification and high sensitivity analysis of heparan sulfate from cells and tissues: Toward glycomics profiling. *J. Biol. Chem.* **2009**, *284*, 25714–25722. [[CrossRef](#)]
37. Wasteson, A. A method for the determination of the molecular weight and molecular-weight distribution of chondroitin sulphate. *J. Chromatogr.* **1971**, *59*, 87–97. [[CrossRef](#)]
38. Deakin, J.A.; Lyon, M. A simplified and sensitive fluorescent method for disaccharide analysis of both heparan sulfate and chondroitin/dermatan sulfates from biological samples. *Glycobiology* **2008**, *18*, 483–491. [[CrossRef](#)]
39. Holley, R.J.; Ellison, S.M.; Fil, D.; O'Leary, C.; McDermott, J.; Senthivel, N.; Langford-Smith, A.W.; Wilkinson, F.L.; D'Souza, Z.; Parker, H.; et al. Macrophage enzyme and reduced inflammation drive brain correction of mucopolysaccharidosis IIIB by stem cell gene therapy. *Brain* **2018**, *141*, 99–116. [[CrossRef](#)]
40. Dubaissi, E.; Rousseau, K.; Lea, R.; Soto, X.; Nardeosingh, S.; Schweickert, A.; Amaya, E.; Thornton, D.J.; Papalopulu, N. A secretory cell type develops alongside multiciliated cells, ionocytes and goblet cells, and provides a protective, anti-infective function in the frog embryonic mucociliary epidermis. *Development* **2014**, *141*, 1514–1525. [[CrossRef](#)]